The Journal of Neuroscience, August 15, 2002, 22(16):6962–6971

Mitochondrial Ca^{2+} Uptake Regulates the Excitability of Myenteric Neurons

Pieter Vanden Berghe, James L. Kenyon, and Terence K. Smith

Department of Physiology and Cell Biology, University of Nevada, School of Medicine, Reno, Nevada 89557-0046

We investigated the role of mitochondria in the regulation of intracellular Ca^{2+} ($[Ca^{2+}]_i$) and excitability of myenteric neurons in guinea pig ileum, using microelectrodes and fura-2 $[Ca^{2+}]_i$ measurements. In AH/Type-II neurons, action potentials evoke ryanodine-sensitive increases in $[Ca^{2+}]_i$ that activate Ca^{2+}-dependent K^+ channels and slow afterhyperpolarizations (AH) lasting ~15 sec. Exposure to the protonophore carbonyl cyanide *p*-(trifluoromethoxy)phenylhydrazone (FCCP; 1 μM) had no significant effect on the membrane potential or resting $[Ca^{2+}]_i$. However, action potentials elicited in the presence of FCCP triggered a sustained (>5 min) increase in $[Ca^{2+}]_i$ and a compound hyperpolarization (13.4 ± 1.5 mV). The respiratory chain blockers antimycin A and rotenone (10 μM) had similar effects that developed more slowly. Depletion of the intracellular Ca^{2+} stores with thapsigargin (2 μM) or ryanodine (10 μM) greatly attenuated the hyperpolarization caused by FCCP. S/Type-I neurons that do not have AH were hyperpolarized by mitochondrial inhibition independently of action potentials. Blockade of the F_0F_1 ATPase by oligomycin (10 μM) had variable effects on myenteric neurons. The majority of AH/Type-II neurons were hyperpolarized by oligomycin, most likely by activating ATP-dependent K^+ channels. This hyperpolarization was not triggered by action potential firing and not accompanied by an increase in $[Ca^{2+}]_i$. MitoTracker staining revealed a dense mitochondrial network particularly in myenteric AH/Type-II neurons, supporting the importance of mitochondrial Ca^{2+} buffering in this subset of neurons. The data indicate that mitochondrial uptake of Ca^{2+} released from the endoplasmic reticulum sets $[Ca^{2+}]_i$ and the activity of Ca^{2+}-dependent conductances, thus regulating the excitability of myenteric neurons.

Key words: mitochondria; fura-2; intracellular calcium; MitoTracker; ER tracker; neuron; K_{Ca} channel; K_{ATP} channel; afterhyperpolarization; neuronal excitability; antimycin A; FCCP; rotenone; oligomycin; guinea pig ileum

Mitochondria produce ATP via ATPases that run in reverse, driven by the proton electrochemical gradient across the mitochondrial membrane. This gradient is built up by electron transport during oxidative phosphorylation. Besides their role in supplying energy, mitochondria are also important in apoptosis, aging, and Ca^{2+} homeostasis. Although the latter has long been debated, recent studies have put mitochondria back on the Ca^{2+} scene as crucial players (Duchen, 2000; Friel, 2000; Rizzuto et al., 2000). Friel and Tsien (1994) described a Ca^{2+} store in bullfrog sympathetic neurons that was sensitive to the protonophore FCCP [carbonyl cyanide *p*-(trifluoromethoxy)phenylhydrazone], and mitochondria also have been shown to alter depolarization-induced $[Ca^{2+}]_i$ responses and the gating properties of Ca^{2+}-activated currents in a variety of neurons, indicating substantial Ca^{2+} removal by these organelles (Thayer and Miller, 1990; Werth and Thayer, 1994; Kenyon and Goff, 1998; Nowicky and Duchen, 1998; Pivovarova et al., 1999; Friel, 2000; Vanden Berghe et al., 2002; Wang and Thayer, 2002). Quantitative measurements have revealed a double role for mitochondria: they sequester Ca^{2+} during depolarization to release it again during repolarization (Babcock and Hille, 1998; Colegrove et al., 2000). Several systems, including Ca^{2+} uniporters, Ca^{2+}/H^+ exchangers, Na^+-dependent and independent release mechanisms, and permeability transition pores, contribute to mitochondrial Ca^{2+} handling (Gunter et al., 2000). Further, mitochondria often are positioned closely to the endoplasmic reticulum (ER), and optimal ER function requires competent mitochondria (Landolfi et al., 1998).

Myenteric neurons are comprised in a ganglionated network in the intestinal wall. They include intrinsic sensory neurons, interneurons, and motor neurons that exert reflex activity and coordinate the propulsion of the intestinal contents (Smith et al., 1992). Electrophysiologically, these neurons have been classified in two or more groups (Nishi and North, 1973; Hirst et al., 1974; Wood, 1994; Smith et al., 1999). S/Type-I neurons have either phasic or tonic firing characteristics and their action potentials are TTX-sensitive. The AH/Type-II neurons are characterized by prolonged afterhyperpolarizations (AH) that follow action potential firing. Their action potentials have, besides the TTX-sensitive part, also a Ca^{2+} component (Morita et al., 1982; Hirst et al., 1985) that triggers Ca^{2+} release from the ER via the activation of ryanodine receptors (Hillsley et al., 2000; Vogalis et al., 2001). The increased intracellular Ca^{2+} concentration opens Ca^{2+}-activated K^+ channels responsible for the transient slow AH, a mechanism also observed in other neurons (Kawai and Watanabe, 1989; Sah and McLachlan, 1991; Yoshizaki et al., 1995; Moore et al., 1998; Shah and Haylett, 2000; Vogalis et al., 2002). The AH/Type-II neurons have been identified as intrinsic primary afferent neurons (Furness et al., 1998) and are therefore important in the organization of gastrointestinal motility. By inhibiting the throughput of sensory information during the afterhyperpolarization, they determine the frequency at which interneurons and motor neurons are driven. Because the AH is

Received Feb. 25, 2002; revised May 17, 2002; accepted May 24, 2002.

This work was supported by National Institute of Diabetes and Digestive and Kidney Diseases Grant PO1 DK-41315. P.V.B. is a postdoctoral Fellow of the Fund for Scientific Research (FWO, Flanders, Belgium).

Correspondence should be addressed to Dr. T. K. Smith, Department of Physiology and Cell Biology/352, University of Nevada, School of Medicine, Reno, NV 89557-0046. E-mail: tks@physio.unr.edu.

directly dependent on the $[Ca^{2+}]_i$ and because there is evidence that mitochondria play an important role in the Ca^{2+} handling in several other neurons, we aimed to investigate the role of mitochondria in the Ca^{2+} homeostasis and therefore the membrane excitability of myenteric neurons.

Parts of this work have been published previously as an abstract (Vanden Berghe and Smith, 2001).

MATERIALS AND METHODS

Tissue preparation. Adult guinea pigs (250–350 gm) were asphyxiated by CO_2, followed by exsanguination (a method approved by the Animal Ethics Committee at the University of Nevada, Reno). A 5 cm segment of ileum was removed, flushed with cold Krebs' solution, and pinned flat in a Sylgard-lined dissection dish. The intestine was opened along the serosal border, and the mucosa, submucosa, and circular muscle layer were removed with fine forceps. During the dissection the preparation was perfused constantly with ice-cold Krebs' solution bubbled with a 3% CO_2/97% O_2 gas mixture. The longitudinal muscle myenteric plexus preparations were stretched and clipped on a stainless steel ring. The tissues were equilibrated in a recording dish with a coverslip bottom for at least 1 hr in warmed Krebs' solution (36°C; bubbled with 3% CO_2/97% O_2). Shortly after the temperature reached steady state, vigorous contractions were observed in the tissue preparations. To make intracellular recordings possible, we added 1–2 μM nicardipine and 1 μM atropine to the bath solution to relax the underlying longitudinal muscle layer (Hillsley et al., 2000).

Membrane potential recordings. Ganglia were identified easily under bright-field light microscopy (Nikon TE 300; Nikon, Tokyo, Japan). The neurons were impaled with glass microelectrodes pulled on a 767 Sutter (Novato, CA) Microelectrode puller, and the membrane potential was recorded. To perform $[Ca^{2+}]_i$ measurements simultaneously, we filled the tips of the electrodes with 1–2 mM bis-fura-2 (K_D = 370 nM) hexapotassium salt dissolved in 1–2 M KCl. The rest of the electrode was filled with 2 M KCl. The resistance of the electrodes varied between 120 and 150 MΩ. The signals were amplified with an Axoclamp 2B amplifier (Axon Instruments, Union City, CA) and monitored continuously on a Tektronix R468 oscilloscope (Tektronix, Beaverton, OR). A bipolar electrode was used to stabilize the tissue against the coverslip bottom and to elicit synaptic potentials in the impaled neurons. Intracellular pulses and extracellular pulse trains were triggered and generated by a Master-8 pulse generator (A.M.P.I., Jerusalem, Israel).

Fura-2 measurements of $[Ca^{2+}]_i$. Fura-2 was loaded iontophoretically into the neurons by applying a train of hyperpolarizing pulses (0.2–0.4 nA at 1–2 Hz) for 2–4 min. Fluorescent signals were recorded with an Ionoptix (Milton, MA) Fluorescence System. A xenon lamp was used as a UV light source. Differential excitation (340/380 nm) of the Ca^{2+} indicator resulted from a spinning chopper wheel (at 60 Hz) to obtain ratiometric values at 30 Hz. Images were recorded with a CCD camera (Ionoptix), and rectangular regions of interest were drawn in the image. The fura-2 ratio was calculated for that specific area. The membrane potential recordings were sampled at the maximal rate (1 kHz) simultaneously with the fura-2 signals by using the analog-to-digital board of the Ionoptix interface box and displayed and stored in the same data file. We chose to express the $[Ca^{2+}]_i$ signals as fura-2 ratios rather than calibrated Ca^{2+} signals, because the R_{min} could not be obtained reliably from calibrations by using ionomycin and 0 mM Ca^{2+} solutions. This was in part due to the way the preparation was set up and also attributable to the fact that the underlying muscle layer interfered with exact calibration of the signals.

Immunochemical stainings and fluorescent markers. Myenteric plexus longitudinal muscle preparations were pinned flat in sterile Sylgard-lined dissection dishes. The tissues were incubated (37°C; 5% CO_2) during 1 hr in the presence of 0.1–1 μM ER-Tracker Blue DPX and/or 0.1–1 μM MitoTracker Green. The organotypic medium consisted of HAM/F12 culture medium supplemented with 2% fetal bovine serum, 1 μM nifedipine, and 1% penicillin–gentamycin antibiotic solution. The tissues were washed thoroughly in cold Krebs' solution, fixed in 4% paraformaldehyde (30 min), and washed in a 0.1 M PO_4^{3-} buffered 0.9% NaCl solution, pH 7.2. To identify calbindin-like immunoreactive neurons, we incubated the tissues (48 hr) in a 0.1 M PO_4^{3-} buffered 0.9% NaCl solution, pH 7.2, containing 1:100 mouse monoclonal anti-calbindin D-28K antibody. The secondary antibody was anti-mouse IgG coupled to Texas Red (1:150; 90 min). The tissues were washed and mounted on slides with Aquamount. An Olympus BX50 microscope with specific filter cubes (FITC: EX, BP470/490; DM, 505; EM, BA 535/50; and aminomethylcoumarin: EX, D360/40; DM, BS 400 dichroic longpass; EM, BA 435–485; Chroma, Brattleboro, VT) was used to visualize the MitoTracker and ER tracker, respectively. Confocal imaging was performed with Bio-Rad (Hercules, CA) MRC 600 (60× lens) and Nikon confocal microscopes (40× lens). Images were acquired via excitation wavelengths of 488 nm (for MitoTracker Green) and 568 nm (for Texas Red). Scion Image (Frederick, MD) was used to quantify MitoTracker intensity in composite images of *z*-series scans of five optical sections through a depth of 2.5 μm, using a confocal aperture <20% of maximum.

Calculations and statistics. Amplitudes and durations of the transient events were calculated as indicated in Figure 1. The time to 90% recovery was calculated as a measurement of duration (90% duration) of the afterhyperpolarization and the Ca^{2+} transient. Resting membrane potentials were measured before and during the application of mitochondrial blockers and compared with a paired Student's *t* test or ANOVA with a Bonferroni test as a *post hoc* analysis. To study the effect of mitochondrial blockers on the transient responses, we calculated both the 90% duration and the remaining amplitude of the AH and Ca^{2+} transient 15 sec after action potential spiking. The average ± SEM duration and amplitudes of AH and Ca^{2+} transients were compared with a paired Student's *t* test. A *p* value of 0.05 was considered the cutoff for statistical significance; *n* values specify the number of neurons. Curve fittings and statistical analysis were performed in GraphPad Prism (San Diego, CA) or MS Excel (Microsoft, Redmond, WA).

Drugs and solutions. All drugs and the antibody against calbindin were obtained from Sigma (St. Louis, MO). Bis-fura-2 hexapotassium salt, MitoTracker Green, and ER-Tracker Blue DPX were obtained from Molecular Probes (Eugene, OR). The anti-mouse IgG coupled to Texas Red was from Vector Labs (Burlingame, CA), and tissue culture supplies (HAM/F12, fetal bovine serum, and antibiotics) were obtained from Invitrogen (Grand Island, NY). The Krebs' solution used throughout this study contained (in mM): 120.3 NaCl, 5.9 KCl, 1.2 $MgCl_2$, 1.2 NaH_2PO_4, 15.5 $NaHCO_3$, 2.5 $CaCl_2$, and 11.5 glucose.

RESULTS

Microelectrode recordings were obtained from 102 neurons (75 animals), 54 of which were identified as AH/Type-II neurons on the basis of the prominent AH they displayed after action potential (AP) firing. Most of the hyperpolarizations consisted of both a fast (fAH) and a slow (sAH) component (Fig. 1*A,B*). The average amplitude of the sAH, elicited by 2 APs, was 9.8 ± 0.6 mV, and the average 90% duration was 15.9 ± 2.9 sec (n = 10). fAH values were smaller (5.1 ± 0.3 mV) and shorter (43.5 ± 1.5 msec). The amplitudes of both fast and slow AH and the duration of the sAH increased linearly ($r^2 > 0.9$) with the number of action potentials preceding the AH (fAH, ~2.5 mV/AP; sAH, ~2 mV/AP; DUR_{sAH}, 2.2 sec/AP; n = 6). Single APs usually did not elicit a detectable fAH. The amplitude of the sAH was also linearly dependent ($r^2 > 0.85$) on the holding potential (current clamp) and increased ~1 mV for each 10 mV the neuron was depolarized. In 13 AH neurons the $[Ca^{2+}]_i$ was monitored simultaneously. The sAH was always closely matched by a Ca^{2+} transient that started with the AP firing and reached a maximum 385 ± 81 msec (n = 7) after onset of the depolarizing pulse. The sAH itself reached its maximum 1115 ± 257 msec (n = 7) after the onset of AP firing (Fig. 1*A*). The amplitude and duration of the accompanying Ca^{2+} transient, like for those of the AH, increased for an increasing number of action potentials (Fig. 2*A*), and the recovery followed an exponential time course (τ = ~2.4 sec) similar to that described in a previous report (Hillsley et al., 2000).

In phasic S/Type-I neurons the $[Ca^{2+}]_i$ increased gradually during the repetitive firing of single APs (up to 10) and decayed slowly afterward (Fig. 2*B*). Single APs never elicited a detectable transient in these neurons. The Ca^{2+} transients in tonically firing S/Type-I neurons increased in amplitude with the number of APs

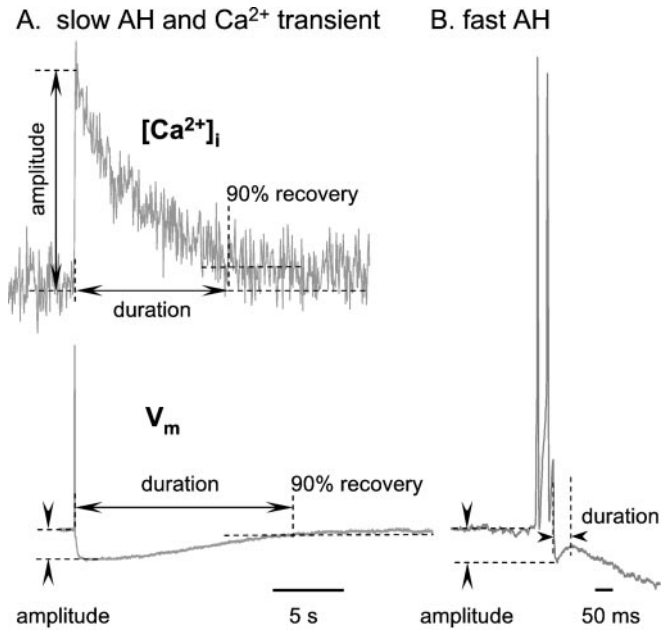

Figure 1. Schematic overview of some parameters calculated in this study. *A*, A slow afterhyperpolarization (sAH) and the matching Ca^{2+} transient. Amplitude and 90% duration were calculated as indicated with the *dashed lines*. *B*, Amplitude and duration of the fast afterhyperpolarization (fAH).

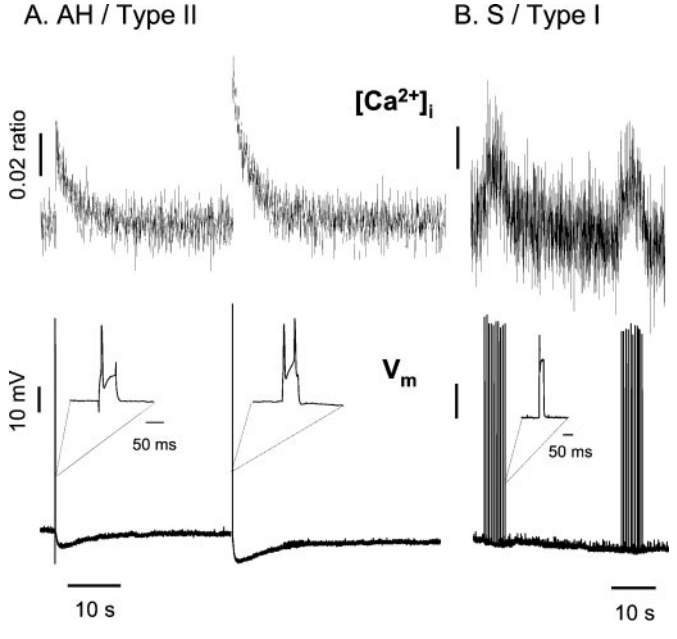

Figure 2. A typical example of the responses as observed in myenteric neurons. *Top panels* show the changes in $[Ca^{2+}]_i$; *bottom panels* are the changes in membrane potential (V_m). *A*, Action potential firing in AH/Type-II neurons is followed by a transient afterhyperpolarization that is larger for an increasing number of action potentials, as shown in the *insets*. The afterhyperpolarization is matched closely by a $[Ca^{2+}]_i$ transient, which decays exponentially. *B*, In S/Type-I neurons several action potentials are needed to elicit a detectable Ca^{2+} transient that is increasing and decaying gradually.

during the depolarizing pulse, whereas the short afterhyperpolarization (3.5 ± 0.3 sec) that sometimes was observed in these neurons (Shuttleworth and Smith, 1999) was independent of the number of APs.

Effect of mitochondrial inhibitors on membrane potential and $[Ca^{2+}]_i$ of AH/Type-II neurons

Membrane potential and resting $[Ca^{2+}]_i$

To assess the effect of mitochondrial inhibition on neuronal excitability, we challenged nine AH neurons with the protonophore FCCP (1 μM). The membrane potential was measured in control conditions and in the presence of FCCP before and after stimulation. Exposure to FCCP (~1.5 min) did not change the resting membrane potential significantly (−57.5 ± 4.2 to −59.2 ± 4.3 mV; ANOVA; Bonferroni *post hoc* analysis; $p > 0.05$; $n = 9$). However, when APs were elicited in the presence of FCCP, the AH triggered by these APs was followed by a significant compound hyperpolarization (−57.5 ± 4.2 to −71.6 ± 4.9 mV; ANOVA; Bonferroni *post hoc* analysis; $p < 0.001$; $n = 9$) (Fig. 3*A*). In the majority (6 of 9) of AH neurons the membrane potential did not recover after the first AH and stayed hyperpolarized. The time to reach the maximum of the compound hyperpolarization was, on average, 146 ± 31 sec ($n = 9$). In the course of this hyperpolarization depolarizing current pulses no longer elicited action potentials (Fig. 3*A*). In six AH neurons in which the $[Ca^{2+}]_i$ was monitored simultaneously, the AP-induced compound hyperpolarization in the presence of FCCP was accompanied by a ~10% increase in fura-2 ratio (0.94 ± 0.13 to 1.04 ± 0.17; $p = 0.04$). This $[Ca^{2+}]_i$ rise was approximately twice the amplitude of the single AP-induced transients (Fig. 3*A*). Seven recordings were kept sufficiently long to investigate the reversibility of FCCP. After washout (5–10 min) the membrane potential recovered to control levels (−61.3 ± 6.7 compared with −57.5 ± 4.2 mV; ANOVA; Bonferroni *post hoc* analysis; $p > 0.05$; $n = 7$). Similarly, after washout of FCCP the $[Ca^{2+}]_i$ no longer was elevated significantly (ratio, 1.11 ± 0.23 to 1.05 ± 0.19; $n = 4$; $p = 0.3$) (Fig. 3*A*).

To check the specificity of FCCP, we used two respiratory chain blockers, antimycin and rotenone, to block mitochondrial function. Similar to the effect of FCCP, antimycin (10 μM) and rotenone (10 μM) induced a compound hyperpolarization that was enhanced by AP firing. Antimycin caused a 6.9 ± 2.2 mV ($n = 4$) hyperpolarization, reaching its maximal amplitude in 450 ± 30 sec, and rotenone hyperpolarized the membrane 9.8 ± 3.8 mV ($n = 3$) in 255 ± 25 sec (Fig. 3*B,C*). The hyperpolarization in the presence of the respiratory chain blockers, however, never developed as rapidly as in FCCP. None of the three mitochondrial inhibitors had a detectable effect on the shape and duration of the APs.

AH and Ca^{2+} transient characteristics

We examined the properties of the AH and associated Ca^{2+} transients during mitochondrial blockade; only those neurons were included with an AH elicited by the same number of APs in control and drug conditions. The amplitude of both the AH (11.6 ± 1.1 to 10.4 ± 1.2 mV; $p = 0.01$; $n = 4$) and the accompanying Ca^{2+} transient were reduced (ratio, 0.077 ± 0.016 to 0.053 ± 0.011; $p = 0.01$; $n = 4$) in the presence of FCCP. When clamped back to the predrug resting membrane potential, the AH amplitude remained smaller (Fig. 3*A*, *inset*). Although the 90% duration of the AH and Ca^{2+} transients was prolonged ($n = 3$), relevant statistical analysis of the AH duration was not possible because in four of seven neurons the AH did not recover and merged continuously into the compound hyperpolarization induced by FCCP. To quantify the change in recovery, we measured the hyperpolarization 15 sec (the average 90% duration of the AH) after action potential firing. The neurons were hyper-

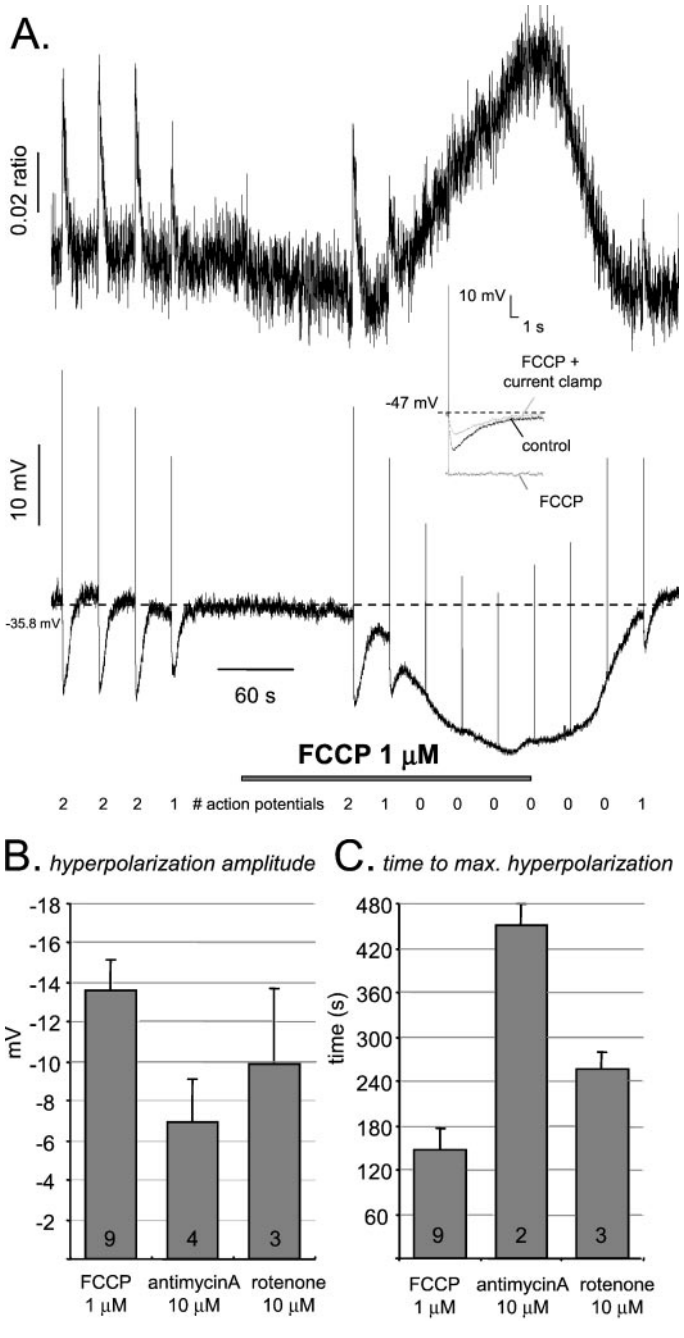

Figure 3. Effect of mitochondrial blockers on the membrane potential and $[Ca^{2+}]_i$ of AH/Type-II neurons. *A*, Typical example of the effect of FCCP on an AH/Type-II neuron. The compound hyperpolarization induced by FCCP is triggered and amplified by action potential firing. The *number* of action potentials that are elicited is indicated under each stimulus. The *top trace* represents the $[Ca^{2+}]_i$ changes, whereas the membrane potential is shown in the *bottom panel* of *A*. The presence of FCCP (1 μM) is indicated with a *horizontal bar*. The *inset* shows a membrane potential recording from another neuron in control conditions (*black*), in the presence of FCCP (*dark gray*), and during current clamp in the presence of FCCP (*light gray*). Although clamped to the control potential, the amplitude of the AH remains reduced in FCCP. *B*, The average amplitude ± SEM of the compound hyperpolarization induced by FCCP, antimycin A, and rotenone in AH/Type-II neurons. *C*, The average time ± SEM to reach the maximum hyperpolarization. The number of neurons per condition is indicated in the bars.

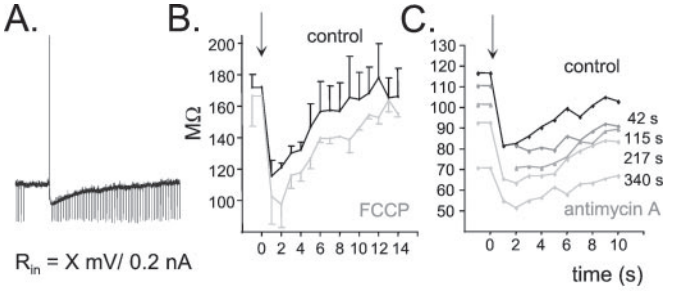

Figure 4. The effect of FCCP (1 μM) and antimycin (10 μM) on the input resistance changes during the slow afterhyperpolarization in AH/Type-II neurons. *A*, The input resistance (R_{in}) is calculated by measuring the voltage deflection (*X*) for a fixed current step (0.2 nA) and is inversely dependent on the number of open channels in the membrane. *B*, The R_{in} (MΩ) during the first 15 sec of the AH in normal conditions (*black*) and in the presence of FCCP (*gray*). The *data points* are averages ± SEM of two to four trials in three neurons. The *arrow* at time 0 sec indicates the time of the action potential. *C*, The R_{in} (MΩ) in control (*black*) and in the presence of antimycin A (*gray*). Individual traces were measured at different time points (as indicated) after the start of the antimycin application. The *arrow* at time 0 sec indicates the time of the action potential.

polarized significantly more in the presence of FCCP (2.0 ± 1.4 to 5.3 ± 1.8 mV; $p = 0.04$; $n = 7$), and the residual Ca^{2+} elevation was increased slightly (ratio, 0.005 ± 0.003 to 0.011 ± 0.003; $p = 0.02$; $n = 4$).

Antimycin A did not significantly alter the amplitude of the AH (8.7 ± 2 to 7.9 ± 1.8 mV; $p = 0.19$; $n = 4$), but the 90% duration was prolonged by ~40%. Similarly, the amplitude of the AH was not altered by rotenone (7.2 ± 1.6 to 9.7 ± 0.9 mV; $p = 0.37$; $n = 3$), and the 90% duration increased, with one neuron that never recovered. Similar to the hyperpolarizing effect of the respiratory chain blockers, the effect on the AH was slower and less pronounced than that of FCCP. Also, unlike FCCP, a prolonged exposure to rotenone and antimycin was required for the drug to become fully effective. None of the mitochondrial blockers altered the properties of the fast AH.

Input resistance

The AH that follows an action potential in myenteric neurons is caused by K^+ efflux through Ca^{2+}-dependent K^+ channels (Hirst et al., 1985; Vogalis et al., 2002). Depending on the neuron type, the Ca^{2+} responsible for opening of these channels originates directly from the extracellular space or indirectly from the intracellular Ca^{2+} stores (Berridge, 1998). In myenteric neurons the Ca^{2+}-induced Ca^{2+} release from ryanodine-sensitive stores provides the bulk of Ca^{2+} responsible for this afterhyperpolarization (Hillsley et al., 2000). The opening of K^+ channels leads to a decrease in input resistance (R_{in}), which can be monitored by measuring the amplitude of the voltage deflection elicited by a constant hyperpolarizing current pulse (Fig. 4*A*). We set out to monitor the changes in R_{in} during the AH, which is regulated by the opening and gradual closure of Ca^{2+}-activated K^+ channels. Single hyperpolarizing pulses were given every second before and during the AH. During the AH the R_{in} dropped to 70% of the resting R_{in}, whereas in the presence of FCCP (1 μM) it dropped to almost 50% (Fig. 4*B*). Similarly, although the effect developed more slowly, the drop in R_{in} was enhanced by antimycin A and was more pronounced for longer exposure times (69.8, 60.8, 55.2, and 45.6% for 42, 115, 217, and 340 sec of exposure, respectively) (Fig. 4*C*). The input resistance also was measured at the time the compound hyperpolarization in the presence of FCCP reached

its maximum. Surprisingly, this compound hyperpolarization was not accompanied by a decrease in general R_{in} when measured at the maximal FCCP effect (113 ± 30 compared with 92 ± 18 MΩ; $n = 6$; $p = 0.16$), suggesting the inhibition of other conductances.

Role of intracellular Ca^{2+} stores

To investigate the contribution of Ca^{2+} release from the intracellular Ca^{2+} stores, we performed some experiments after the depletion of the Ca^{2+} stores with thapsigargin (Tg) and during the blockade of ryanodine (Ry) receptors, shown to be crucial for the myenteric AH (Hillsley et al., 2000; Vogalis et al., 2001). The blockade of the ATP-dependent Ca^{2+} pump with Tg did not have major effects on the membrane potential (~5 mV depolarization in 30 min) but abolished the AH. The compound hyperpolarization caused by FCCP was attenuated greatly by Tg. Indeed, in three Tg-treated neurons FCCP did not cause a significant hyperpolarization (−59.6 ± 8.4 to −65.9 ± 6.8 mV; $p = 0.07$) even when APs were fired (Fig. 5*A*). In two neurons a small depolarization developed after 3 min of FCCP exposure during the next 10 min.

In preliminary experiments the AH neurons were perfused with Ry for at least 200 sec before exposure to FCCP. Here FCCP still induced a significant AP-dependent hyperpolarization (−54.0 ± 3.9 to −61.7 ± 5.5; $n = 3$; $p = 0.03$) (Fig. 5*B*). The amplitude of the compound hyperpolarization was not different from that of FCCP alone (Fig. 5*C*); however, the presence of Ry significantly delayed the effect (360 ± 121 compared with 146 ± 31 sec; $p = 0.03$) (Fig. 5*D*). This may indicate that Ca^{2+} release from Ry receptors is needed to accelerate the hyperpolarizing effect of FCCP. To test this hypothesis, we exposed neurons to Ry for >30 min, shown to reduce the AH to 40% (Hillsley et al., 2000). Similar to the Tg treatment, in Ry-treated neurons ($n = 3$) FCCP no longer evoked a hyperpolarization (−61.3 ± 3.9 to −67.0 ± 1.8 mV; $p = 0.22$) even in the presence of AP firing.

Effect of mitochondrial inhibitors on the membrane potential and $[Ca^{2+}]_i$ of S/Type-I neurons

S/Type-I neurons are heterogeneous in terms of firing characteristics, including phasic S neurons, having only 1 AP for a prolonged (100–500 msec) depolarization pulse, and tonic S neurons, with multiple spikes. The effect of mitochondrial inhibition was studied in 29 S/Type-I neurons (23 phasic and 6 tonic). All S/Type-I neurons were pooled because no consistent differences in the effect of mitochondrial inhibitors were observed between the two types of S neurons (Fig. 6*A*). FCCP (1 μM) significantly hyperpolarized S/Type-I neurons (−57.0 ± 3.9 to −67.9 ± 5.5 mV; $p = 0.02$; $n = 6$) in 189 ± 42 sec. However, this hyperpolarization differed from that observed in AH neurons in that it developed independently of AP firing (Fig. 6*A*). The respiratory chain blocker rotenone caused a similar hyperpolarization (−54.1 ± 3.6 to −65.4 ± 2.4 mV; $p = 0.04$; $n = 4$) (Fig. 6*B*), but it took longer for the hyperpolarization to develop fully (271 ± 73 sec) (Fig. 6*C*). The complex I blocker antimycin hyperpolarized three of eight S/Type-I neurons (−43.0 ± 8.7 to −65.7 ± 4.6 mV; $p = 0.03$) in 280 ± 53 sec (Fig. 6*B,C*) and had no effect on the other S/Type-I neurons (−51.8 ± 5.1 to −51.2 ± 5.9 mV; $p = 0.5$). Within the limits of detection none of the mitochondrial inhibitors had an effect on the shape of the APs of these neurons.

In 12 S/Type-I neurons the $[Ca^{2+}]_i$ was monitored simultaneously during the application of mitochondrial blockers. The link between $[Ca^{2+}]_i$ and membrane potential changes was not as clear in S/Type-I neurons as for AH/Type-II neurons (see also Shuttleworth and Smith, 1999; Hillsley et al., 2000). Although some changes in $[Ca^{2+}]_i$ were observed in the presence of FCCP, on average the $[Ca^{2+}]_i$ levels were not significantly different at the time the hyperpolarization reached its maximum (0.91 ± 0.11 to 0.95 ± 0.13; $n = 5$; $p = 0.09$). Similarly, antimycin and rotenone

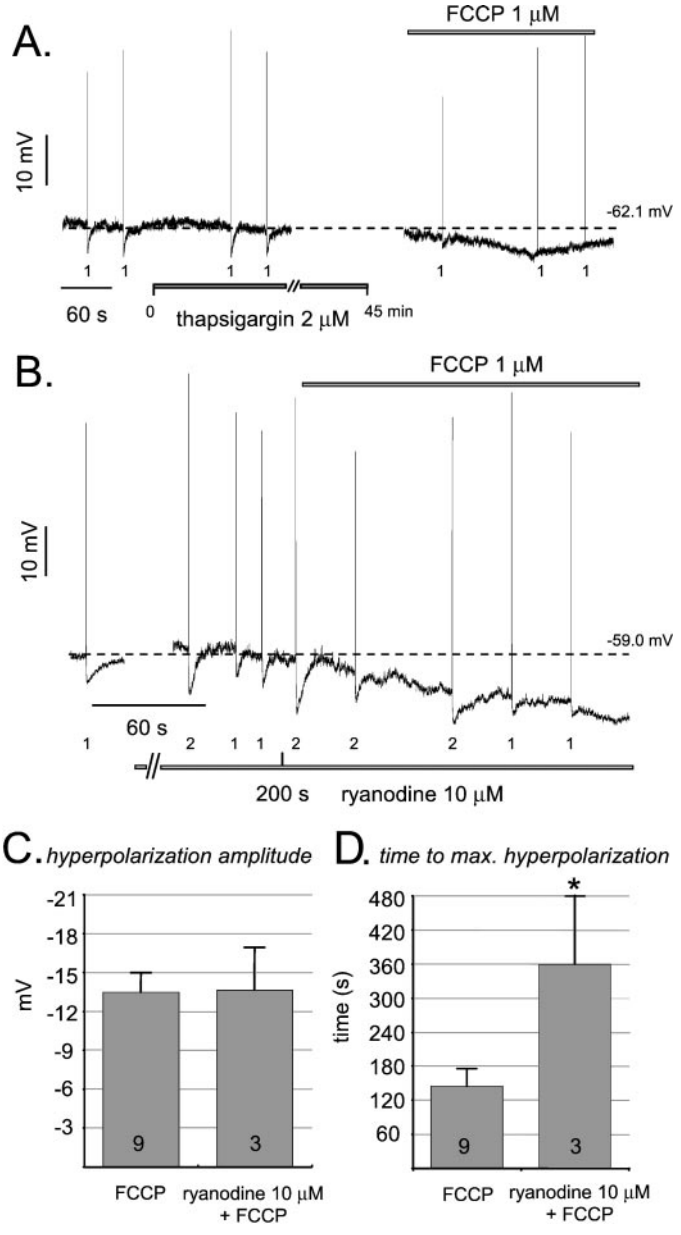

Figure 5. The involvement of intracellular Ca^{2+} stores in the effect of FCCP on AH/Type-II neurons. Drugs are added as indicated by the *horizontal bars*; the *number* of action potentials that are elicited is indicated under each stimulus. *A*, Effect of FCCP after blockade of the ATP-dependent Ca^{2+} pump with thapsigargin (2 μM). The AH is abolished almost completely after the thapsigargin treatment. Action potentials in the presence of FCCP induce only a small hyperpolarization. *B*, The effect of FCCP in the presence of ryanodine (10 μM). Ryanodine was applied 200 sec before the addition of FCCP. The FCCP-induced hyperpolarization develops slower than in the absence of ryanodine. *C*, The average amplitude ± SEM of the hyperpolarization induced by FCCP alone and in the presence of ryanodine. *D*, The average time ± SEM to reach the maximum hyperpolarization. In the presence of ryanodine the hyperpolarizing effect of FCCP is delayed significantly. The number of neurons per condition is indicated in the bars. Significant differences ($p < 0.05$) are indicated with an *asterisk*.

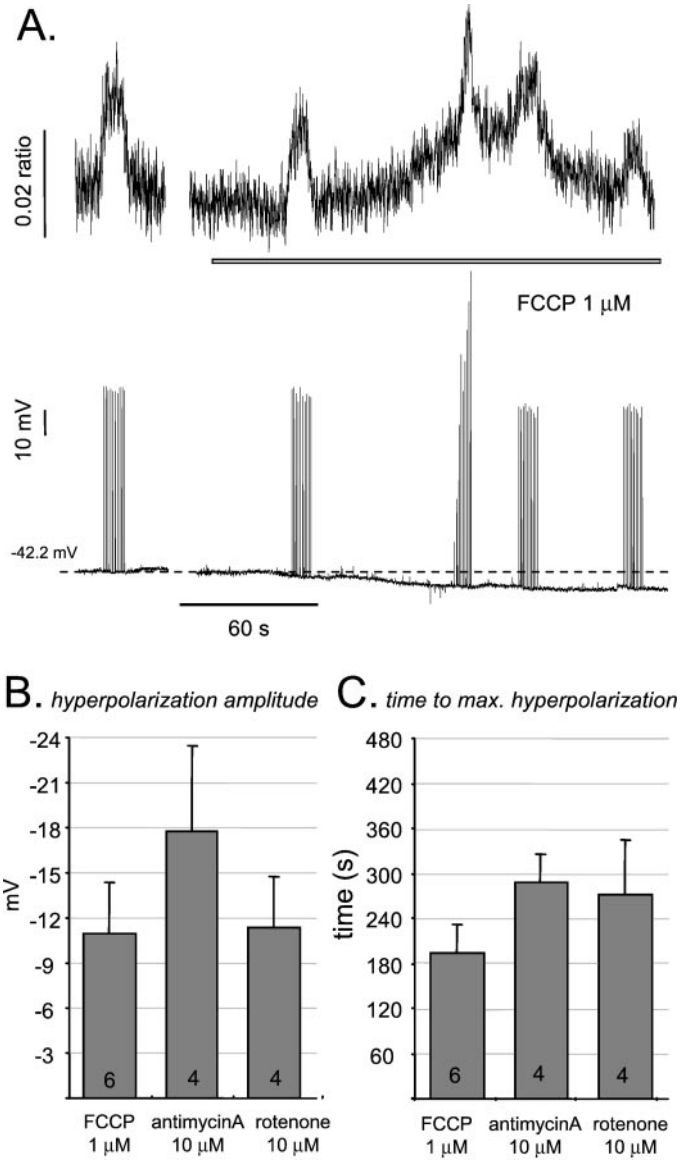

Figure 6. Effect of mitochondrial blockers on the membrane potential and $[Ca^{2+}]_i$ of S/Type-I neurons. *A*, Typical example of the effect of FCCP on an S/Type-I neuron. The hyperpolarization develops slowly and is independent of action potential firing. The *top trace* represents the $[Ca^{2+}]_i$ changes, whereas the membrane potential is shown in the *bottom panel* of *A*. The presence of FCCP (1 μM) is indicated with a *horizontal bar*. *B*, The average amplitude ± SEM of the hyperpolarization induced by FCCP, antimycin A, and rotenone in S/Type-I neurons. *C*, The average time ± SEM to reach the maximum hyperpolarization. The number of neurons per condition is indicated in the bars.

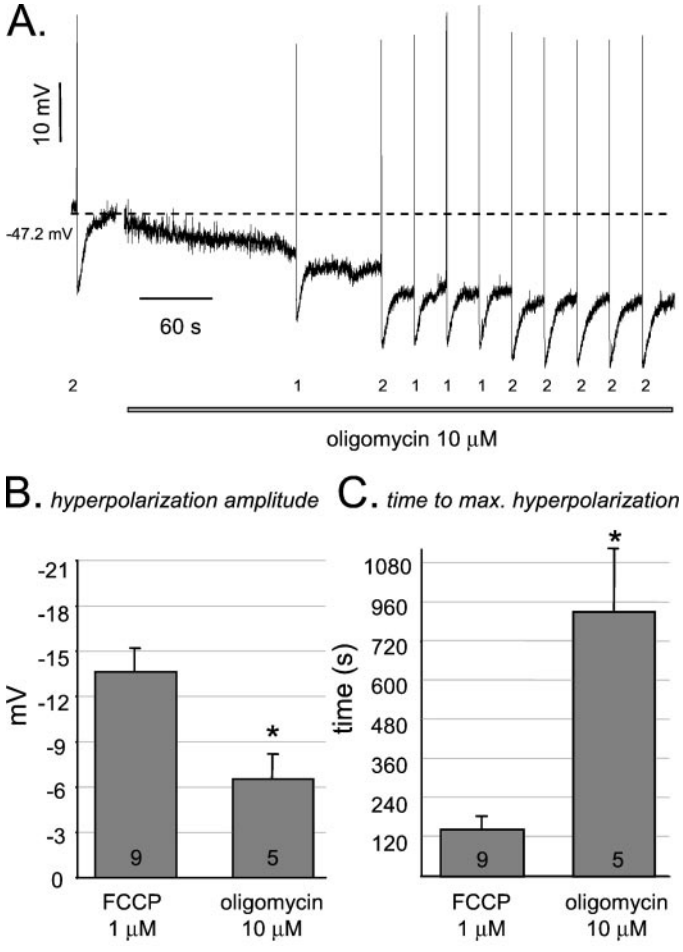

Figure 7. The effect of the mitochondrial F_0F_1 ATPase blocker oligomycin (10 μM) and FCCP on the membrane potential of AH/Type-II neurons. Oligomycin is added as indicated by the *horizontal bar*; the *number* of action potentials that are elicited is indicated under each stimulus. *A*, Oligomycin hyperpolarizes the membrane potential of AH/Type-II neurons. The hyperpolarization develops slowly and is not triggered by action potential firing. *B*, The average amplitude ± SEM of the hyperpolarization. *C*, Average time ± SEM to reach the maximum hyperpolarization induced by oligomycin compared with the effect of FCCP. The number of neurons per condition is indicated in the bars. Significant differences ($p < 0.05$) are indicated with an *asterisk*.

did not cause a significant $[Ca^{2+}]_i$ increase in S/Type-I neurons. The mitochondrial blockers did not alter significantly the AP-induced Ca^{2+} transients elicited in S/Type-I neurons.

Effect of F_0F_1 ATPase blockade on the membrane potential and $[Ca^{2+}]_i$ in myenteric neurons

During mitochondrial blockade the ATP/ADP balance may change because of the lack of ATP production or ATP consumption by the depolarized mitochondria. Oligomycin (10 μM) blocks the mitochondrial F_0F_1 ATPase and therefore can be used to assess the contribution of ATP depletion. In five of seven AH neurons oligomycin induced a membrane hyperpolarization (−50.5 ± 3.9 to −57.1 ± 4.3 mV; $p = 0.01$) that was not influenced by AP firing (Fig. 7*A*) and not accompanied by a $[Ca^{2+}]_i$ rise. This hyperpolarization was smaller (Fig. 7*B*) and developed significantly slower than the FCCP-induced compound hyperpolarization (800 ± 183 compared with 146 ± 31 sec; $p = 0.005$; $n = 5$) (Fig. 7*C*). In two other AH neurons a small depolarization (~5 mV) was observed. Oligomycin did not alter the amplitude and duration of the AH ($n = 5$). Oligomycin had no detectable effect on the AP of AH/Type-II neurons. In four AH neurons that were hyperpolarized with FCCP, we added the K_{ATP} blocker glibenclamide (1 μM) at least 6 min after the addition of FCCP. The hyperpolarized neurons partially recovered (from −76.6 ± 6.4 to −67.9 ± 5.2 mV; ANOVA; $p < 0.01$ in FCCP; control, −66.6 ± 6.3 before FCCP), indicating the involvement of a K_{ATP} conductance. Blockade of the F_0F_1 ATPase in S/Type-I neurons had variable effects; four of seven neurons hyperpolarized slowly (−48.9 ± 3.7 to −58.8 ± 3.8 mV in 420 ± 100 sec), whereas in three others a depolarization (~7 mV) was ob-

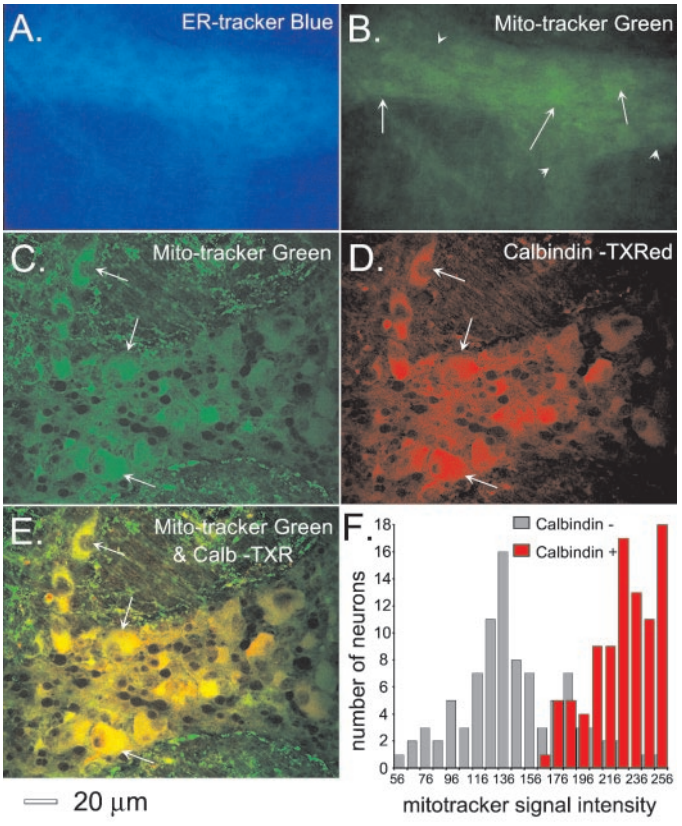

Figure 8. Endoplasmic reticulum (ER) tracker, MitoTracker, and calbindin-like immunostaining in whole-mount myenteric plexus preparations; scale bar, 20 μm. *A*, ER-Tracker Blue DPX was used to visualize the ER in the myenteric plexus. Note that ER-Tracker Blue DPX shows an overall staining of the ganglion and the underlying layers. *B*, MitoTracker Green was used to stain mitochondria in the same ganglion. The MitoTracker staining shows a different pattern, in that some neurons in the ganglion are brighter (*arrows*) than others (*arrowheads*). *C–E*, Confocal images of a MitoTracker (*C*) calbindin (*D*) double staining. The preparations were stained with MitoTracker Green and processed afterward with a primary antibody against calbindin and a secondary antibody coupled to Texas Red. *E*, The calbindin-like immunoreactive neurons (e.g., *arrows*) were stained intensely with MitoTracker, as clearly seen in the overlay of *C* and *D*. *F*, Distribution histogram of the MitoTracker intensity for calbindin-like immunoreactive neurons (*red*) and calbindin-negative neurons (*gray*). The MitoTracker signal is clearly higher in calbindin-like immunoreactive neurons.

served. Oligomycin did not induce a rise in $[Ca^{2+}]_i$ in S/Type-I neurons ($n = 3$).

MitoTracker, ER tracker, and immunohistochemical stainings

Longitudinal muscle myenteric plexus preparations were stained with ER tracker and MitoTracker (Fogarty et al., 2000; Buckman et al., 2001) to visualize the ER and the mitochondria in the myenteric neurons of the guinea pig ileum. Because the myenteric plexus consists of a monolayer of neurons, we used conventional fluorescence microscopy. Out-of-focus light, emerging from the continuous underlying muscle layer, equally contributed to the whole field and therefore did not affect the assessment of organelle tracker dyes in different myenteric neurons. Although ER tracker images showed an overall staining of the preparation, the myenteric neurons stained brighter than the underlying muscle layer (Fig. 8*A*). Unlike the ER tracker staining, the intensity of MitoTracker staining (Fig. 8*B*) was higher in a certain subset of neurons (Fig. 8*B*, *arrows*) in the myenteric plexus. To identify this subset of neurons, we used an antibody against calbindin, a calcium-binding protein that is a marker for AH/Type-II neurons in various tissues (Iyer et al., 1988; Song et al., 1991; Furness et al., 1998). Confocal microscopy was used to examine preparations that were double labeled with MitoTracker (Fig. 8*C*) and the calbindin antibody (Fig. 8*D*). This revealed a colocalization between calbindin-like immunoreactivity and intense MitoTracker staining (Fig. 8*E*). In Figure 8*F* the MitoTracker intensity is plotted as a histogram for both calbindin-positive and calbindin-negative neurons, clearly indicating that calbindin-positive neurons have a more intense MitoTracker staining (Fig. 8*F*).

DISCUSSION

In this study we combined intracellular recordings and Ca^{2+} imaging to assess the effect of mitochondrial blockers on resting membrane potential and excitability of myenteric neurons of the guinea pig ileum. Mitochondria are important organelles not only because they are the major source of energy but also because they play a crucial role in Ca^{2+} homeostasis. Here we showed that the resting membrane potential and therefore the excitability of myenteric neurons, in particular AH/Type-II neurons, are regulated in part by Ca^{2+} uptake via mitochondria.

The AH/Type-II neurons displayed a double-phased afterhyperpolarization after AP firing. The slow phase was mirrored by a transient increase and exponential decay in $[Ca^{2+}]_i$, closely linked to the afterhyperpolarization in amplitude and duration (Tatsumi et al., 1988; Hillsley et al., 2000; Vogalis et al., 2000). Hirst et al. (1985) suggested that the delay observed at the onset of the slow AH was attributable to a Ca^{2+} priming period of the K^+ channels that were involved, whereas Vogalis et al. (2001) attributed the delay to a transient inward current, unmasked by TEA and blocked by niflumic acid.

The blockade of mitochondria hyperpolarized both S/Type-I and AH/Type-II myenteric neurons. In AH/Type-II neurons the resting membrane potential was not altered significantly by FCCP until action potentials were elicited. Then the action potentials and the AH were followed by a compound hyperpolarization that lasted for several minutes. Simultaneous $[Ca^{2+}]_i$ recordings showed that the compound hyperpolarization in AH neurons was accompanied by a rise in $[Ca^{2+}]_i$, suggesting that mitochondria sequester an important amount of Ca^{2+} during normal neuronal function. However, unlike the observations in rat hippocampal neurons (Nowicky and Duchen, 1998), the rise in $[Ca^{2+}]_i$ did not develop in the absence of activation. In line with other reports (Greenwood et al., 1997; Pivovarova et al., 1999) the FCCP effect was reversible, and both membrane potential and $[Ca^{2+}]_i$ recovered during washout. In contrast to AH/Type-II neurons, the FCCP induced hyperpolarization in S/Type-I neurons developed steadily and independently of AP firing. To test whether the effect of FCCP was specific, we also used other mitochondrial blockers, rotenone and antimycin A, blocking complex I and III, respectively, of the respiratory chain. Hyperpolarizations of similar amplitude were observed in both S/Type-I and AH/Type-II neurons. In AH/Type-II neurons AP firing enhanced the effect, similar to that of FCCP.

The effect of mitochondrial blockers on AH and $[Ca^{2+}]_i$ transient characteristics was studied in those neurons without an immediate compound hyperpolarization. FCCP reduced the AH and the accompanying Ca^{2+} transient. Several studies report increased $[Ca^{2+}]_i$ responses to activation during mitochondrial blockade in different neuronal preparations (Khodorov et al.,

1999; Pivovarova et al., 1999; Friel, 2000; Wang and Thayer, 2002). However, in cultured myenteric neurons mitochondrial blockade did not affect the amplitude of K^+-induced Ca^{2+} transients but slowed the $[Ca^{2+}]_i$ decay (Vanden Berghe et al., 2002). In the present study, as well, mitochondrial blockade by FCCP significantly prolonged the duration of the Ca^{2+} transient. All of the effects on the Ca^{2+} transients invariably were reflected in effects on the AH. In the presence of FCCP the AH was smaller, but the time to reach the maximum and the total duration were increased. These findings indicate that hampered Ca^{2+} removal prolongs the $[Ca^{2+}]_i$ elevation and therefore delays the closure of Ca^{2+}-activated channels. Similar observations for Ca^{2+}-activated currents were made in smooth muscle cells (Greenwood et al., 1997), chick DRG neurons (Kenyon and Goff, 1998), and rat hippocampal neurons (Nowicky and Duchen, 1998). More evidence for this prolonged opening of Ca^{2+}-activated K^+ channels was found in the R_{in} measurements. Mitochondrial blockers amplified the drop in R_{in} during the AH. However, by the time the compound hyperpolarization reached its maximum, the R_{in} had recovered to control levels. Therefore, the compound hyperpolarization cannot be attributed simply to an increase in K^+ conductance, unless another conductance is switched off accordingly. A possible candidate is I_h (Galligan et al., 1990; Rugiero et al., 2002), a cation current activated during hyperpolarization, which is reduced by metabolic inhibition and increases in $[Ca^{2+}]_i$ (Duchen, 1990).

Because mitochondria act both as a source and sink, the net effect on Ca^{2+} uptake is probably highly dependent on the kinetics of the blockade and the state of the mitochondria (Gunter et al., 2000). This also might explain why the AH and Ca^{2+} transient amplitude are affected differently by FCCP and rotenone. Also, the fact that the hyperpolarizing effect and the reduction in R_{in} by FCCP developed faster and more suddenly than for antimycin and rotenone was probably attributable to the mechanism of the action of the drugs. The latter two block the respiratory cycle and therefore inhibit mitochondrial function more slowly than the sudden collapse of mitochondrial potential induced by FCCP.

The importance of AH/Type-II neuronal intracellular Ca^{2+} stores was assessed with ryanodine and thapsigargin, an irreversible blocker of the ATP-dependent Ca^{2+} pump. Depletion of the ER with thapsigargin prevented the AP-induced compound hyperpolarization in the presence of FCCP. Similarly, prolonged exposure to Ry, shown to reduce the AH significantly (Hillsley et al., 2000), eliminated the compound hyperpolarization. Even short treatment with Ry already delayed the FCCP hyperpolarization without affecting the amplitude. The Ca^{2+} release from ryanodine-sensitive Ca^{2+} stores seems to be prerequisite for FCCP to exert its effect, proving that mitochondria normally buffer substantial amounts of the Ca^{2+} release from the ER in myenteric AH/Type-II neurons.

Although the maximal hyperpolarization induced by mitochondrial blockade was similar in S/Type-I neurons and AH/Type-II, in the former the hyperpolarization was independent of AP firing. This suggested that another mechanism is responsible for the hyperpolarization in S/Type-I neurons and maybe also in unstimulated AH neurons. To assess the contribution of the putative changes in cytosolic ATP/ADP ratio attributable to the mitochondrial blockade, we blocked the F_0F_1 ATPase with oligomycin. Oligomycin itself hyperpolarized the majority of AH neurons and had variable effects on S neurons. The hyperpolarization developed independently of AP firing rather than in

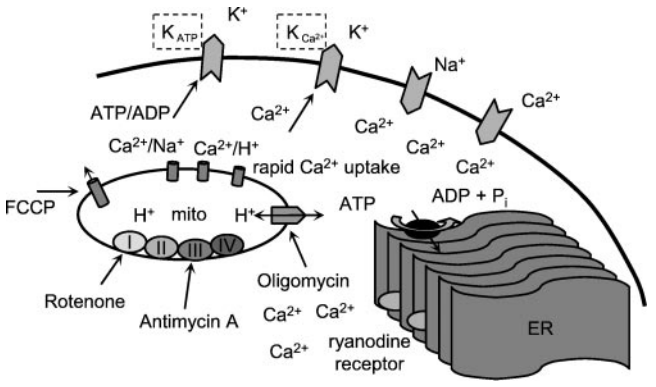

Figure 9. Schematic representation of the Ca^{2+} handling in myenteric neurons. Action potential firing causes Ca^{2+} entry through voltage-activated Ca^{2+} channels. The increase in $[Ca^{2+}]_i$ is amplified by the release of Ca^{2+} from the ER via activation of ryanodine receptors (Hillsley et al., 2000). Functional mitochondria sequester Ca^{2+} and thereby lower the $[Ca^{2+}]_i$. A blockade of the mitochondria results in a prolonged elevation of the $[Ca^{2+}]_i$, which in turn causes a prolonged activation of the Ca^{2+}-dependent conductances. On the other hand, ATP depletion, occurring during mitochondrial blockade or the inhibition of the F_0F_1 ATPase by oligomycin, may activate K_{ATP} channels, thus leading to a Ca^{2+}-independent hyperpolarization.

FCCP. Also, the $[Ca^{2+}]_i$ did not rise during oligomycin, which led to the idea that a Ca^{2+}-independent mechanism, probably based on the activation of ATP-sensitive K^+ channels, was involved (Otero and Carrasco, 1984; Roper and Ashcroft, 1995; Hyllienmark and Brismar, 1996). Glibenclamide, a blocker of K_{ATP}, partially restored the membrane potential in myenteric neurons that were hyperpolarized in FCCP. Liu et al. (1999) also presented evidence for such a K_{ATP} current in myenteric neurons by showing that glucose deprivation induced a tolbutamide-sensitive hyperpolarization. They also showed that the subunits of the K_{ATP} channel ($Kir_{1.6}$ and sulfonylurea receptor) were present in both calbindin-positive and other myenteric neurons. It is not clear what determines the different responses to oligomycin. Especially for S/Type-I neurons, different subtypes (phasic/tonic) and underlying differences in energy requirement may cause the variable effects. In AH neurons a shortage of ATP also may, besides activating K_{ATP}, slow down the ATP-dependent Ca^{2+} uptake by the ER (Landolfi et al., 1998).

In this study we also used fluorescent tracker molecules to trace mitochondria and ER in the myenteric plexus. The ER tracker stained the whole tissue, with a more extensive staining of the myenteric plexus. MitoTracker showed a more patterned staining, in which some neurons were brighter than others. In a double-labeling experiment the neurons with intensive MitoTracker staining were identified as calbindin-positive AH/Type-II neurons. This suggested that AH/Type-II neurons had a higher number or a denser mitochondrial network. Electron microscopy data showing that calbindin-positive neurons, unlike the calbindin-negative neurons, had numerous electron-dense mitochondria (Pompolo and Furness, 1988) corroborate our findings. These data tie in well with the physiological observations that in AH/Type-II neurons the effect of mitochondrial blockers is more pronounced than in S/Type-I neurons.

In conclusion, the blockade of mitochondria triggers a series of events in AH/Type-II neurons involving several currents (Fig. 9). First, the Ca^{2+} released from ER is not buffered efficiently by the impaired mitochondria, slowing the deactivation of Ca^{2+}-dependent K^+ conductances and leading to a prolongation of the

AH. Second, the glibenclamide data imply that ATP-sensitive K^+ channels also are activated in the course of the compound hyperpolarization. This mechanism is likely to explain the oligomycin-induced hyperpolarization that develops without a $[Ca^{2+}]_i$ rise. Further, the recovery of R_{in} at the peak of the compound hyperpolarization implies the inhibition of a nonselective cation current. The contribution of these different conductances probably varies throughout the course of the compound hyperpolarization. In an early stage, action potential firing and consecutive ER Ca^{2+} release trigger the Ca^{2+}-dependent component of the compound hyperpolarization. However, the ATP-dependent component also might be set off because, in an attempt to remove the excess Ca^{2+} ions, activated neurons might consume the remaining ATP more rapidly. Although mitochondrial blockade hyperpolarizes both types of myenteric neurons, the effects on S/Type-I neurons are less pronounced and not triggered by activation. It has to be noted that the S/Type-I neurons are a mixed population, comprising descending and ascending interneurons and inhibitory and excitatory motor neurons. Although the link between their function and the electrical properties is not established clearly, it is likely that functional differences are reflected in their electrical and Ca^{2+} handling properties. Mitochondria are highly sensitive to oxidative stress and therefore may be important in the pathological responses during inflammation. Reactive oxygen species induced fluctuations in the membrane potential of colonic AH myenteric neurons (Wada-Takahashi and Tamura, 2000). In view of the results in this study, it is likely that mitochondrial dysfunction and therefore disabled Ca^{2+} sequestration underlie the initial hyperpolarizations.

REFERENCES

Babcock DF, Hille B (1998) Mitochondrial oversight of cellular Ca^{2+} signaling. Curr Opin Neurobiol 8:398–404.

Berridge MJ (1998) Neuronal calcium signaling. Neuron 21:13–26.

Buckman JF, Hernandez H, Kress GJ, Votyakova TV, Pal S, Reynolds IJ (2001) MitoTracker labeling in primary neuronal and astrocytic cultures: influence of mitochondrial membrane potential and oxidants. J Neurosci Methods 104:165–176.

Colegrove SL, Albrecht MA, Friel DD (2000) Quantitative analysis of mitochondrial Ca^{2+} uptake and release pathways in sympathetic neurons. Reconstruction of the recovery after depolarization-evoked $[Ca^{2+}]_i$ elevations. J Gen Physiol 115:371–388.

Duchen MR (1990) Effects of metabolic inhibition on the membrane properties of isolated mouse primary sensory neurones. J Physiol (Lond) 424:387–409.

Duchen MR (2000) Mitochondria and Ca^{2+} in cell physiology and pathophysiology. Cell Calcium 28:339–348.

Fogarty KE, Kidd JF, Turner A, Skepper JN, Carmichael J, Thorn P (2000) Microtubules regulate local Ca^{2+} spiking in secretory epithelial cells. J Biol Chem 275:22487–22494.

Friel DD (2000) Mitochondria as regulators of stimulus-evoked calcium signals in neurons. Cell Calcium 28:307–316.

Friel DD, Tsien RW (1994) An FCCP-sensitive Ca^{2+} store in bullfrog sympathetic neurons and its participation in stimulus-evoked changes in $[Ca^{2+}]_i$. J Neurosci 14:4007–4024.

Furness JB, Kunze WA, Bertrand PP, Clerc N, Bornstein JC (1998) Intrinsic primary afferent neurons of the intestine. Prog Neurobiol 54:1–18.

Galligan JJ, Tatsumi H, Shen KZ, Surprenant A, North RA (1990) Cation current activated by hyperpolarization (I_H) in guinea pig enteric neurons. Am J Physiol 259:966–972.

Greenwood IA, Helliwell RM, Large WA (1997) Modulation of Ca^{2+} activated Cl^- currents in rabbit portal vein smooth muscle by an inhibitor of mitochondrial Ca^{2+} uptake. J Physiol (Lond) 505[Pt 1]:53–64.

Gunter TE, Buntinas L, Sparagna G, Eliseev R, Gunter K (2000) Mitochondrial calcium transport: mechanisms and functions. Cell Calcium 28:285–296.

Hillsley K, Kenyon JL, Smith TK (2000) Ryanodine-sensitive stores regulate the excitability of AH neurons in the myenteric plexus of guinea pig ileum. J Neurophysiol 84:2777–2785.

Hirst GD, Holman ME, Spence I (1974) Two types of neurones in the myenteric plexus of the duodenum in the guinea pig. J Physiol (Lond) 361:297–314.

Hirst GD, Johnson SM, van Helden DF (1985) The slow calcium-dependent potassium current in a myenteric neurone of the guinea pig ileum. J Physiol (Lond) 361:315–337.

Hyllienmark L, Brismar T (1996) Effect of metabolic inhibition on K^+ channels in pyramidal cells of the hippocampal CA1 region in rat brain slices. J Physiol (Lond) 496[Pt 1]:155–164.

Iyer V, Bornstein JC, Costa M, Furness JB, Takahashi Y, Iwanaga T (1988) Electrophysiology of guinea pig myenteric neurons correlated with immunoreactivity for calcium binding proteins. J Auton Nerv Syst 22:141–150.

Kawai T, Watanabe M (1989) Effects of ryanodine on the spike afterhyperpolarization in sympathetic neurones of the rat superior cervical ganglion. Pflügers Arch 413:470–475.

Kenyon JL, Goff HR (1998) Temperature dependencies of Ca^{2+} current, Ca^{2+}-activated Cl^- current, and Ca^{2+} transients in sensory neurones. Cell Calcium 24:35–48.

Khodorov B, Pinelis V, Storozhevykh T, Yuravichus A, Khaspekhov L (1999) Blockade of mitochondrial Ca^{2+} uptake by mitochondrial inhibitors amplifies the glutamate-induced calcium response in cultured cerebellar granule cells. FEBS Lett 458:162–166.

Landolfi B, Curci S, Debellis L, Pozzan T, Hofer AM (1998) Ca^{2+} homeostasis in the agonist-sensitive internal store: functional interactions between mitochondria and the ER measured *in situ* in intact cells. J Cell Biol 142:1235–1243.

Liu M, Seino S, Kirchgessner AL (1999) Identification and characterization of glucoresponsive neurons in the enteric nervous system. J Neurosci 19:10305–10317.

Moore KA, Cohen AS, Kao JP, Weinreich D (1998) Ca^{2+}-induced Ca^{2+} release mediates a slow post-spike hyperpolarization in rabbit vagal afferent neurons. J Neurophysiol 79:688–694.

Morita K, North RA, Tokimasa T (1982) The calcium-activated potassium conductance in guinea pig myenteric neurones. J Physiol (Lond) 329:341–354.

Nishi S, North RA (1973) Intracellular recording from the myenteric plexus of the guinea pig ileum. J Physiol (Lond) 231:471–491.

Nowicky AV, Duchen MR (1998) Changes in $[Ca^{2+}]_i$ and membrane currents during impaired mitochondrial metabolism in dissociated rat hippocampal neurons. J Physiol (Lond) 507[Pt 1]:131–145.

Otero MJ, Carrasco L (1984) Action of oligomycin on cultured mammalian cells. Permeabilization to translation inhibitors. Mol Cell Biochem 61:183–191.

Pivovarova NB, Hongpaisan J, Andrews SB, Friel DD (1999) Depolarization-induced mitochondrial Ca accumulation in sympathetic neurons: spatial and temporal characteristics. J Neurosci 19:6372–6384.

Pompolo S, Furness JB (1988) Ultrastructure and synaptic relationships of calbindin-reactive, Dogiel type II neurons, in myenteric ganglia of guinea pig small intestine. J Neurocytol 17:771–782.

Rizzuto R, Bernardi P, Pozzan T (2000) Mitochondria as all-round players of the calcium game. J Physiol (Lond) 529[Pt 1]:37–47.

Roper J, Ashcroft FM (1995) Metabolic inhibition and low internal ATP activate K-ATP channels in rat dopaminergic substantia nigra neurones. Pflügers Arch 430:44–54.

Rugiero F, Gola M, Kunze WA, Reynaud JC, Furness JB, Clerc N (2002) Analysis of whole-cell currents by patch clamp of guinea pig myenteric neurones in intact ganglia. J Physiol (Lond) 538:447–463.

Sah P, McLachlan EM (1991) Ca^{2+}-activated K^+ currents underlying the afterhyperpolarization in guinea pig vagal neurons: a role for Ca^{2+}-activated Ca^{2+} release. Neuron 7:257–264.

Shah M, Haylett DG (2000) Ca^{2+} channels involved in the generation of the slow afterhyperpolarization in cultured rat hippocampal pyramidal neurons. J Neurophysiol 83:2554–2561.

Shuttleworth CW, Smith TK (1999) Action potential-dependent calcium transients in myenteric S neurons of the guinea pig ileum. Neuroscience 92:751–762.

Smith TK, Bornstein JC, Furness JB (1992) Convergence of reflex pathways excited by distension and mechanical stimulation of the mucosa onto the same myenteric neurons of the guinea pig small intestine. J Neurosci 12:1502–1510.

Smith TK, Burke EP, Shuttleworth CW (1999) Topographical and electrophysiological characteristics of highly excitable S neurones in the myenteric plexus of the guinea pig ileum. J Physiol (Lond) 517:817–830.

Song ZM, Brookes SJ, Costa M (1991) Identification of myenteric neurons which project to the mucosa of the guinea pig small intestine. Neurosci Lett 129:294–298.

Tatsumi H, Hirai K, Katayama Y (1988) Measurement of the intracellular calcium concentration in guinea pig myenteric neurons by using fura-2. Brain Res 451:371–375.

Thayer SA, Miller RJ (1990) Regulation of the intracellular free calcium concentration in single rat dorsal root ganglion neurones *in vitro*. J Physiol (Lond) 425:85–115.

Vanden Berghe P, Smith TK (2001) Mitochondrial Ca^{2+} uptake regu-

lates after-hyperpolarizations in guinea-pig myenteric neurons. Gastroenterology 120:A200.
Vanden Berghe P, Missiaen L, Janssens J, Tack J (2002) Calcium signaling and removal mechanisms in cultured myenteric neurons. Neurogastroenterol Motil 14:63–73.
Vogalis F, Hillsley K, Smith T (2000) Recording ionic events from cultured, DiI-labeled myenteric neurons in the guinea pig proximal colon. J Neurosci Methods 96:25–34.
Vogalis F, Furness JB, Kunze WA (2001) Afterhyperpolarization current in myenteric neurons of the guinea pig duodenum. J Neurophysiol 85:1941–1951.
Vogalis F, Harvey JR, Furness JB (2002) TEA- and apamin-resistant K_{Ca} channels in guinea pig myenteric neurons: slow AHP channels. J Physiol (Lond) 538:421–433.
Wada-Takahashi S, Tamura K (2000) Actions of reactive oxygen species on AH/Type 2 myenteric neurons in guinea pig distal colon. Am J Physiol Gastrointest Liver Physiol 279:G893–G902.
Wang GJ, Thayer SA (2002) NMDA-induced calcium loads recycle across the mitochondrial inner membrane of hippocampal neurons in culture. J Neurophysiol 87:740–749.
Werth JL, Thayer SA (1994) Mitochondria buffer physiological calcium loads in cultured rat dorsal root ganglion neurons. J Neurosci 14:348–356.
Wood JD (1994) Physiology of the enteric nervous system. In: Physiology of the gastrointestinal tract (Johnson LR, ed), pp 423–482. New York: Raven.
Yoshizaki K, Hoshino T, Sato M, Koyano H, Nohmi M, Hua SY, Kuba K (1995) Ca^{2+}-induced Ca^{2+} release and its activation in response to a single action potential in rabbit otic ganglion cells. J Physiol (Lond) 486[Pt 1]:177–187.